

Supporting information for:

Understanding the abundance of the rare sugar β -D-allose

G. Juarez,^a E. R. Alonso,^a M. Sanz-Novo,^a J. L Alonso,^a and I. León^{*a}

^aGrupo de Espectroscopía Molecular (GEM), Edificio Quifima, Laboratorios de Espectroscopia y Bioespectroscopia, Unidad Asociada CSIC, Parque Científico UVa, Universidad de Valladolid, 47011 Valladolid, Spain.

***Corresponding Author:**

Iker León Ona, iker.leon@uva.es

phones: +34 983 186345 / +34 983 186349

web: <http://www.gem.uva.es/>

METHODS

Experimental details

D-allose crystallizes only in the β - 4C_1 conformation. Therefore, a commercial sample of β -D-allose (m.p. 160°) was used without any further purification. A solid rod was prepared by pressing the compound's fine powder mixed with a small amount of commercial binder and was placed in the ablation nozzle. A picosecond Nd:YAG laser (266 nm, 12 mJ per pulse, 20 ps pulse width) was used as a vaporization tool. Products of the laser ablation were supersonically expanded using the flow of carrier gas (Ne, 14 bar) and characterized by chirped-pulse Fourier transform microwave spectroscopy (LA-CP-FTMW).¹ Molecular pulses of 800 μ s were used and the generated molecules of allose in the jet were polarised using 4 μ s chirped microwave pulses. After each microwave pulse, four molecular free induction decays (FIDs) were collected for 10 μ s. These FIDs were stored in a fast oscilloscope in the time domain, and Fourier transformed to the frequency domain for analysis. Up to 75000 individual free induction decays at a 2 Hz repetition rate were averaged to obtain the broadband frequency domain spectrum in the 2 to 8^{1–3} and 6 to 14 GHz ranges.^{4,5} The expected accuracy is about 20 kHz.

Theoretical Modeling

In order to guide the experimental characterization, we initially performed a conformational search. As shown in Figure S1, allose can adopt different configurations depending on the orientation of the hydroxymethyl group. The Newman projection indicates the torsion angle as the angle (having an absolute value between 0° and 180°) between bonds to two specified (fiducial) groups, one from the atom nearer (proximal) to the observer and the other from the further (distal) atom.⁶ The resulting conformations around the terminal hydroxymethyl group give rise to the G+ (60°), G- (60°), T (180°), g+ (60°), g- (60°), and t (180°) configurations. We used the symbol cl or cc to describe the clockwise (cl) or counterclockwise (cc) arrangement of the cooperative network of intramolecular hydrogen bonds. Additionally, different intramolecular interactions are expected due to the hydrogen bonds between the hydroxyl groups. Therefore, several conformers are expected. To ease the conformational search, an automated exploration of the intermolecular potential energy surface of the β -D-allose was carried out using fast molecular mechanics methods.⁷ In the second step, geometry optimizations of the lower-energy conformers were done using Gaussian suite programs.⁸ The choice model was the Møller–Plesset (MP2) perturbation theory in the frozen core approximation⁹ and B3LYP density functional including Grimme's dispersions^{10,11} with Becke–Johnson damping,^{12,13} both with the Pople's 6-311++G (d,p) basis set.¹⁴

Figure S1. (a) Haworth projection of β -D-allose. (b) 4C_1 chair conformation. (c) Newman projections around the hydroxymethyl group showing the G-, G+, T, g-, g+ and t configurations.

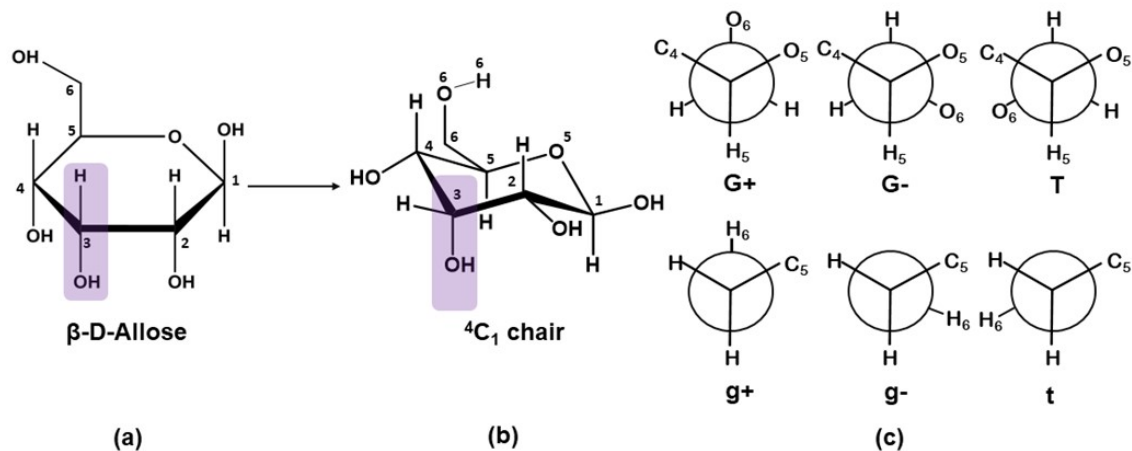


Figure S2. Predicted low-energy conformers of β -D-allose calculated at MP2 and 6-311++G (d,p) basis set. The values indicate the relative energy in cm^{-1} with respect to the global minimum.

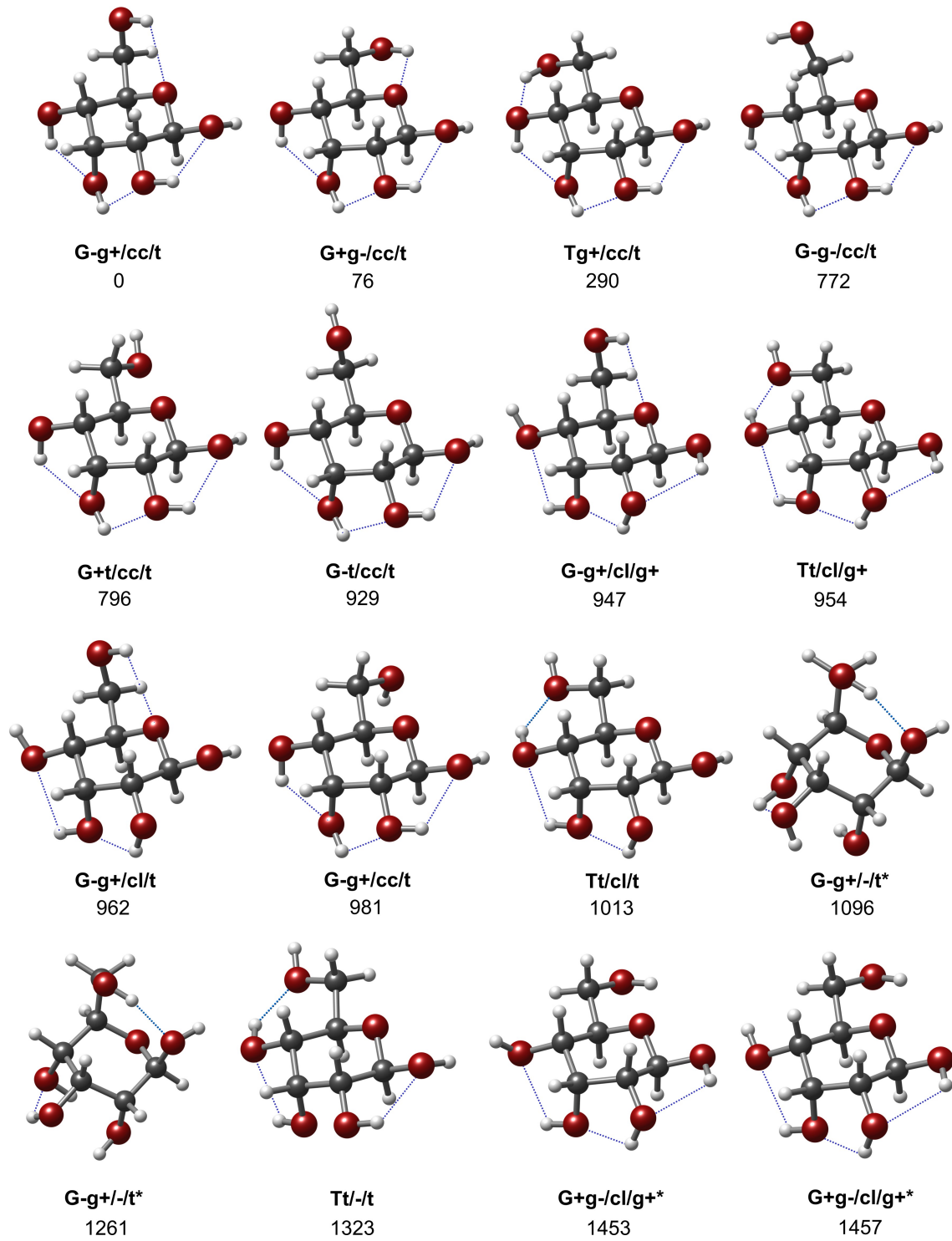


Figure S2. Continuation.

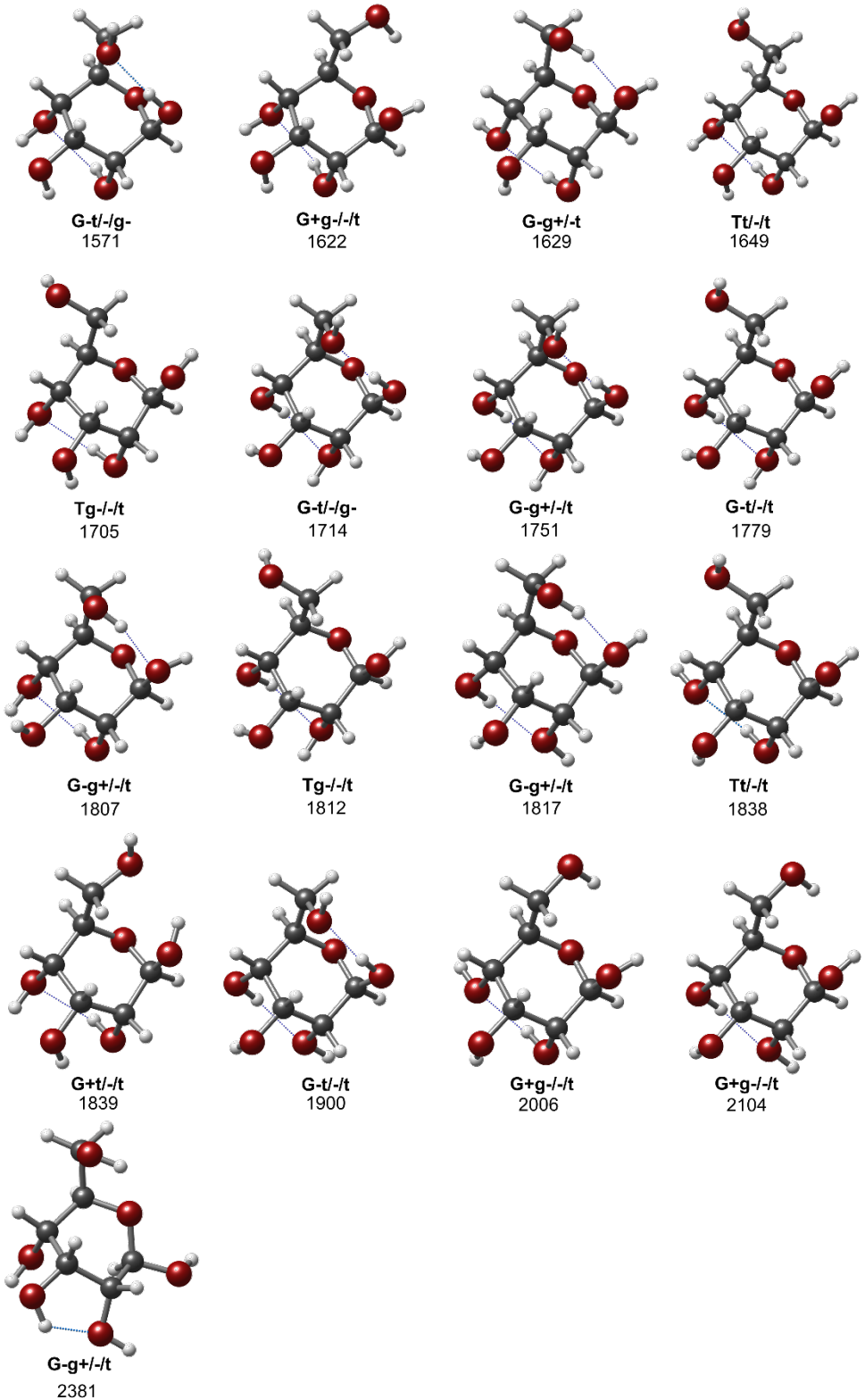


Table S1. Calculated spectroscopic parameters for the lowest energy conformers of β -D-allose. All the calculations were done using MP2 with the Pople's 6-311++G (d,p) basis set. A , B , and C represent the rotational constants (in MHz); μ_a , μ_b , and μ_c are the electric dipole moment components (in D). ΔE is the relative electronic energies (in cm^{-1}) with respect to the global minimum. ΔE_{ZPE} is relative energies (in cm^{-1}) with respect to the global minimum, taking into account the zero point energy. ΔG is the relative energy taking into account the total electronic energy plus the thermal correction to Gibbs free energy (in cm^{-1}) calculated at 298K.

* The structures marked with an asterik are categorized with the same label due to small differences in the geometry that fall within the same category.

Parameters	G-g+/cc/t	G+g-/cc/t	Tg+/cc/t	G-g-/cc/t	G+t/cc/t	G-t/cc/t	G-g+/cl/g+	Tt/cl/g+	G-g+/cl/t
A	1273	1233	1466	1370	1252	1316	1289	1477	1286
B	813	801	723	765	784	793	804	730	802
C	562	534	530	552	534	560	558	530	557
$ \mu_a $	-3.0	2.8	3.3	-1.8	0.2	-0.3	-0.8	-3.4	-2.3
$ \mu_b $	-1.6	-1.5	0.2	0.3	-1.1	-1.4	2.6	0.2	0.9
$ \mu_c $	-2.2	0.4	-0.4	-2.1	-0.1	-2.2	0.3	-0.3	1.6
ΔE	0	103	243	808	958	969	1042	899	1140
ΔE_{ZPE}	0	77	290	773	796	829	947	954	962
ΔG	0	45	320	701	676	735	826	984	787

Parameters	G-g+/cc/t	Tt/cl/t	G-g+/-/t*	G-g+/-/t*	Tt/-/t	G+g-/cl/g+*	G+g-/cl/g+*	G-t/-/g-	G+g-/-/t
A	1254	1467	1262	1258	1489	1230	1223	1262	1410
B	777	729	890	893	724	804	808	894	791
C	530	529	762	760	532	534	534	760	663
$ \mu_a $	1.7	4.8	-1.1	-1.0	-3.4	1.1	0.0	-2.7	0.4
$ \mu_b $	0.0	1.8	1.2	2.0	-3.7	4.2	3.2	-3.1	0.6
$ \mu_c $	1.6	0.7	-1.2	-1.2	-0.4	-1.6	-0.8	0.8	0.2
ΔE	1135	1051	790	956	1349	1541	1571	1300	1512
ΔE_{ZPE}	981	1013	1096	1261	1323	1453	1457	1571	1622
ΔG	868	982	1314	1455	1317	1382	1366	1791	1656

Parameters	G-g+/-/t	Tt/-/t	Tg-/-/t	G-t/-/g-	G+g-/-/t	G-t/-/t	G-g+/-/t	Tg-/-/t	G-g+/-/t
<i>A</i>	1252	1233	1236	1258	1400	1221	1247	1222	1243
<i>B</i>	883	853	847	894	794	862	892	857	889
<i>C</i>	767	670	667	761	663	670	766	668	764
$ \mu_a $	-2.2	2.0	1.4	-2.3	0.7	1.4	-2.0	0.7	-0.9
$ \mu_b $	-0.3	1.6	1.3	-2.3	1.7	2.5	-0.2	2.1	4.5
$ \mu_c $	-3.3	-1.3	1.0	0.8	0.0	-1.3	1.0	1.0	-2.2
ΔE	1495	1632	1594	1462	1642	1751	1609	1695	1694
ΔE_{ZPE}	1629	1649	1705	1714	1751	1779	1807	1812	1817
ΔG	1776	1629	1767	1909	1773	1745	1991	1865	1926

Parameters	Tt/-/t	G+t/-/t	G-t/-/t	G+g-/-/t	G+g-/-/t	G-g+/-/t
<i>A</i>	1223	1451	1245	1389	1382	1170
<i>B</i>	849	803	891	787	793	854
<i>C</i>	675	680	765	667	668	646
$ \mu_a $	3.9	-2.0	-2.7	-1.3	0.2	-1.0
$ \mu_b $	1.0	-1.8	-0.2	-0.8	3.6	2.5
$ \mu_c $	0.3	1.7	-0.5	-1.3	-1.4	1.0
ΔE	1950	1644	1776	2037	2123	2426
ΔE_{ZPE}	1838	1839	1900	2006	2104	2381
ΔG	1772	1994	2055	1981	2075	2235

Table S2. Calculated spectroscopic parameters for the lowest energy conformers of β -D-allose. All the calculations were done using B3LYP density functional including Grimme's dispersion correction with the Pople's 6-311++G (d,p) basis set. A , B , and C represent the rotational constants (in MHz); μ_a , μ_b , and μ_c are the electric dipole moment components (in D). ΔE is the relative electronic energies (in cm^{-1}) with respect to the global minimum. ΔE_{ZPE} is relative energies (in cm^{-1}) with respect to the global minimum, taking into account the zero point energy. ΔG is the relative energy taking into account the total electronic energy plus the thermal correction to Gibbs free energy (in cm^{-1}) calculated at 298K.

Parameters	G-g+/cc/t	G+g-/cc/t	Tg+/cc/t	G+g+/cc/t	G-+/cl/g-	G-g-/cc/t	G+t/cc/t	Tt/cl/g+	Tt/cl/t
A	1256	1222	1453	1253	1249	1348	1244	1463	1451
B	809	794	719	884	887	760	775	724	725
C	557	528	524	754	752	545	527	525	524
$ \mu_a $	3.0	2.8	3.3	1.0	0.9	1.8	0.3	3.4	4.7
$ \mu_b $	1.6	1.5	0.2	0.9	1.7	0.2	1.0	0.2	1.9
$ \mu_c $	2.1	0.4	0.4	1.3	1.2	2.0	0.1	0.3	0.7
ΔE	0	83	66	66	214	826	952	827	906
ΔE_{ZPE}	0	54	116	418	562	764	801	837	879
ΔG	0	24	163	671	795	643	695	857	872

Parameters	G+g+/cc/t	G-T/cc/t	G-g+/cl/g	G-g/cl/t	G-t/cl/g-	Tg+/cl/t	G-t/cl/g-	G-g+/-/t*	G+g-/cc/t
A	1245	1296	1273	1270	1255	1242	1251	1234	1396
B	769	787	798	797	886	879	886	884	787
C	524	554	553	551	750	760	753	757	656
$ \mu_a $	1.6	0.2	-0.9	-2.3	-2.7	-2.0	-2.3	-0.8	0.4
$ \mu_b $	0.0	-1.2	2.4	0.8	3.2	0.5	2.3	-4.2	-0.5
$ \mu_c $	1.5	2.1	0.3	1.6	-0.8	3.3	-0.9	2.2	-0.1
ΔE	1030	1057	1042	1076	636	779	765	1000	1036
ΔE_{ZPE}	895	899	931	933	953	976	1073	1162	1173
ΔG	793	792	809	790	1200	1166	1308	1298	1225

Parameters	G-g+/-/t*	Tt/-/t*	G+g-/-/t*	Tg-/-/t*	G-t/-/g-*	Tt/-/t*	G+g-/-/g+*	G+g-/-g+*	Tg-/-/t
<i>A</i>	1237	1475	1386	1218	1237	1216	1213	1220	1207
<i>B</i>	886	718	789	844	884	849	801	798	852
<i>C</i>	758	527	655	661	757	664	529	528	661
$ \mu_a $	1.9	3.3	0.7	1.5	2.6	2.1	0	1.1	0.8
$ \mu_b $	0.4	3.7	1.6	1.2	0.3	1.5	3.3	4.1	2.0
$ \mu_c $	0.8	0.4	0.1	1.1	0.4	1.2	0.9	1.6	1.0
ΔE	1018	1346	1169	1156	1129	1240	1504	1502	1252
ΔE_{ZPE}	1256	1300	1301	1302	1310	1333	1371	1393	1401
ΔG	1472	1305	1342	1376	1500	1363	1276	1320	1466

Parameters	Tt/-/t*	Tt/-/t*	G+t/-/t*	G+g-/-/t*	G+g-/-/t*	G-g+/-/t*
<i>A</i>	1206	1206	1437	1373	1368	1112
<i>B</i>	857	845	798	782	788	881
<i>C</i>	662	668	673	659	662	692
$ \mu_a $	1.4	3.8	2.0	1.3	0.3	0.2
$ \mu_b $	2.4	1.0	1.9	0.9	3.4	1.9
$ \mu_c $	1.3	0.5	1.7	1.3	1.4	1.0
ΔE	1347	1616	1385	1613	1692	2126
ΔE_{ZPE}	1450	1573	1592	1620	1696	2148
ΔG	1470	1543	1752	1624	1681	1967

Table S3. Measured frequencies and residuals (in MHz) for the rotational transitions of rotamer I using the LA-CP-FTMB spectrometer.

<i>J'</i>	<i>K'</i>_a	<i>K'</i>_c	<i>J''</i>	<i>K''</i>_a	<i>K''</i>_c	<i>v</i>_{obs}	<i>v</i>_{obs} – <i>v</i>_{cal}
3	2	2	2	2	1	4109.065	-0.003
7	4	4	7	3	5	4343.884	-0.008
6	1	5	6	1	6	4353.598	-0.006
6	1	5	6	0	6	4360.495	0.016
2	2	1	1	1	0	4362.007	0.005
3	2	1	2	2	0	4382.723	0.005
3	1	2	2	1	1	4425.971	0.006
2	2	0	1	1	0	4440.417	0.005
7	3	5	7	2	6	4520.138	-0.017
2	2	1	1	1	1	4612.941	0.005
7	5	3	7	4	3	4677.041	-0.024
2	2	0	1	1	1	4691.364	0.018
4	1	3	3	2	2	4715.589	-0.006
4	0	4	3	1	3	4800.796	0.011
4	1	4	3	1	3	4857.034	0.013
6	5	2	6	4	2	4937.746	-0.029
4	0	4	3	0	3	4939.448	-0.024
6	5	1	6	4	2	4942.268	-0.031
4	1	4	3	0	3	4995.734	0.026
6	5	2	6	4	3	5048.371	-0.002
8	5	4	8	4	5	5076.549	0.038
2	2	0	1	0	1	5148.577	0.007
5	2	3	4	3	2	5216.561	0.008
8	3	6	8	2	7	5228.461	-0.009
7	1	6	7	1	7	5267.800	0.023
7	1	6	7	0	7	5269.979	-0.013
7	2	6	7	0	7	5345.901	0.007
5	1	4	4	2	2	5397.078	-0.004
4	2	3	3	2	2	5416.278	0.001
3	1	2	2	0	2	5463.475	0.003
3	2	2	2	1	1	5480.760	0.003
4	3	2	3	3	1	5598.641	0.018
4	3	1	3	3	0	5689.003	0.009
4	1	3	3	1	2	5770.388	0.001
3	2	1	2	1	1	5832.827	0.011
4	2	2	3	2	1	5952.798	0.003
5	0	5	4	1	4	5979.714	0.001
5	1	5	4	1	4	6000.062	-0.012
5	0	5	4	0	4	6035.947	-0.002
5	1	5	4	0	4	6056.312	0.003
3	2	2	2	1	2	6233.568	0.008
5	1	4	4	2	3	6285.673	0.006
3	2	1	2	1	2	6585.637	-0.002
5	2	4	4	2	3	6675.700	0.008
6	2	4	5	3	2	6724.957	0.001
3	2	1	2	0	2	6870.354	0.035
5	1	4	4	1	3	6986.357	-0.001

J'	K'_a	K'_c	J''	K''_a	K''_c	ν_{obs}	$\nu_{\text{obs}} - \nu_{\text{cal}}$
3	3	1	2	2	0	6987.406	-0.002
5	3	3	4	3	2	6992.765	0.005
3	3	0	2	2	0	7003.648	0.002
5	4	2	4	4	1	7021.202	0.010
5	4	1	4	4	0	7042.306	0.001
3	3	1	2	2	1	7065.820	0.003
3	3	0	2	2	1	7082.068	0.012
6	2	4	5	3	3	7099.519	-0.013
6	0	6	5	1	5	7122.240	0.006
6	1	6	5	1	5	7129.118	-0.002
6	0	6	5	0	5	7142.607	0.002
6	1	6	5	0	5	7149.488	0.008
5	3	2	4	3	1	7260.730	0.009
4	2	2	3	1	2	7359.672	0.032
5	2	4	4	1	3	7376.377	0.003
5	2	3	4	2	2	7467.074	0.003
6	2	5	5	2	4	7886.989	-0.005
6	1	5	5	1	4	8093.676	-0.011
7	1	7	6	1	6	8251.654	-0.005
4	3	1	3	2	1	8309.931	0.009
6	3	4	5	3	3	8350.805	0.015
6	4	3	5	4	2	8459.057	0.008
4	3	1	3	2	2	8661.983	0.002
6	2	4	5	2	3	8875.747	0.009
6	3	3	5	3	2	8887.724	-0.005
5	2	3	4	1	3	9056.369	0.042
7	2	6	6	2	5	9058.430	0.010
7	1	6	6	1	5	9165.851	-0.001
8	0	8	7	1	7	9370.914	-0.010
8	1	8	7	1	7	9371.622	0.007
8	0	8	7	0	7	9373.143	0.003
8	1	8	7	0	7	9373.838	0.008
5	1	4	4	0	4	9445.315	-0.011
4	4	1	3	3	0	9560.605	-0.001
4	4	0	3	3	0	9563.377	0.005
4	4	1	3	3	1	9576.832	-0.013
7	3	5	6	3	4	9658.593	-0.008
5	2	4	4	1	4	9779.115	0.008
6	3	4	5	2	3	10126.992	-0.004
7	4	3	6	4	2	10131.968	0.032
7	2	5	6	2	4	10144.837	0.001
8	1	7	7	1	6	10249.918	0.009
9	1	9	8	1	8	10490.670	0.005
9	0	9	8	0	8	10491.149	0.004
8	3	6	7	3	5	10911.175	-0.011
6	2	4	5	1	4	10945.736	0.025
5	4	2	4	3	2	10999.416	0.002
6	3	3	5	2	3	11038.502	-0.004

J'	K'_a	K'_c	J''	K''_a	K''_c	ν_{obs}	$\nu_{\text{obs}} - \nu_{\text{cal}}$
8	6	3	7	6	2	11266.304	-0.019
8	6	2	7	6	1	11270.753	0.007
8	2	6	7	2	5	11274.806	-0.010
8	4	5	7	4	4	11286.100	-0.013
8	5	4	7	5	3	11330.582	-0.011
9	2	8	8	2	7	11332.258	0.012
9	1	8	8	1	7	11350.753	-0.002
8	5	3	7	5	2	11407.445	-0.014
10	1	10	9	1	9	11609.514	-0.014
10	0	10	9	0	9	11609.514	-0.014
8	4	4	7	4	3	11794.063	-0.014
6	3	4	5	2	4	11806.931	-0.021
5	5	1	4	4	0	12104.159	-0.024
5	5	0	4	4	0	12104.602	-0.005
5	5	1	4	4	1	12106.937	-0.012
5	5	0	4	4	1	12107.373	0.001
9	3	7	8	3	6	12113.310	-0.004
9	2	7	8	2	6	12330.150	-0.042
10	1	9	9	2	8	12451.058	0.014
10	2	9	9	2	8	12454.585	-0.002
10	1	9	9	1	8	12461.365	-0.008
10	2	9	9	1	8	12464.899	-0.016
6	4	3	5	3	3	12465.686	-0.019
9	3	7	8	2	6	12514.669	-0.035
6	4	2	5	3	3	12576.304	0.004
11	1	11	10	1	10	12728.169	-0.004
11	0	11	10	0	10	12728.169	-0.004
10	2	8	9	3	7	13199.992	0.021
10	3	8	9	3	7	13276.958	-0.005
9	3	6	8	3	5	13298.509	-0.020
10	2	8	9	2	7	13384.453	-0.049
11	2	10	10	2	9	13574.101	-0.004
11	1	10	10	1	9	13576.467	-0.005
12	1	12	11	1	11	13846.851	-0.009
12	0	12	11	0	11	13846.851	-0.009

Table S4. Measured frequencies and residuals (in MHz) for the rotational transitions of rotamer II.

<i>J'</i>	<i>K'</i>_a	<i>K'</i>_c	<i>J''</i>	<i>K''</i>_a	<i>K''</i>_c	v_{obs}	v_{obs} - v_{cal}
2	2	1	1	1	0	4221.091	0.000
3	2	1	2	2	0	4288.619	0.009
6	1	5	6	1	6	4499.800	0.023
2	2	0	1	1	1	4576.204	-0.005
4	0	4	3	1	3	4598.741	0.025
7	3	5	7	2	6	4600.542	-0.024
4	1	4	3	1	3	4643.366	-0.007
4	0	4	3	0	3	4716.687	0.019
7	4	4	7	2	5	4918.621	0.003
2	2	0	1	0	1	5009.992	0.002
5	2	3	4	3	2	5186.211	-0.008
4	2	3	3	2	2	5236.907	0.013
3	2	2	2	1	1	5282.858	0.007
8	3	6	8	1	7	5372.077	0.011
7	1	6	7	0	7	5421.203	0.015
4	3	2	3	3	1	5443.141	-0.013
4	3	1	3	3	0	5554.447	0.014
4	1	3	3	1	2	5593.745	0.018
5	0	5	4	1	4	5712.174	0.027
5	0	5	4	0	4	5756.815	0.011
5	1	5	4	0	4	5771.925	0.015
4	2	2	3	2	1	5825.127	0.002
5	1	4	4	2	3	6117.877	0.011
4	2	3	3	1	2	6209.554	0.005
5	2	4	4	2	3	6438.497	0.007
3	2	1	2	1	2	6475.910	0.020
5	1	4	4	1	3	6733.698	0.010
3	3	1	2	2	0	6773.352	0.001
5	3	3	4	3	2	6792.510	0.016
6	0	6	5	1	5	6792.958	-0.003
6	1	6	5	1	5	6797.742	0.012
6	0	6	5	0	5	6808.073	0.006
6	1	6	5	0	5	6812.848	0.011
5	4	2	4	4	1	6833.212	0.022
5	4	1	4	4	0	6861.753	0.026
3	3	1	2	2	1	6863.039	-0.021
3	3	0	2	2	1	6883.354	-0.003
5	2	4	4	1	3	7054.320	0.008
5	3	2	4	3	1	7112.483	0.012
5	2	3	4	2	2	7289.002	0.012
6	1	5	5	2	4	7447.957	0.016
6	2	5	5	2	4	7587.888	0.017
6	1	5	5	1	4	7768.584	0.017
7	0	7	6	1	6	7861.024	0.016
7	1	7	6	1	6	7862.448	0.001
7	0	7	6	0	6	7865.782	0.005

<i>J'</i>	<i>K'</i>_a	<i>K'</i>_c	<i>J''</i>	<i>K''</i>_a	<i>K''</i>_c	v obs	v obs - v cal
7	1	7	6	0	6	7867.207	-0.009
6	2	5	5	1	4	7908.502	0.007
6	3	4	5	3	3	8097.840	-0.021
6	4	2	5	4	1	8349.028	-0.006
4	3	1	3	2	2	8456.278	-0.009
6	2	4	5	2	3	8627.801	0.004
7	1	6	6	2	5	8642.464	-0.027
7	2	6	6	2	5	8696.356	0.000
6	3	3	5	3	2	8713.432	0.014
7	1	6	6	1	5	8782.438	0.019
8	1	8	7	1	7	8925.056	0.000
8	0	8	7	0	7	8926.066	-0.008
4	4	0	3	3	1	9300.494	-0.009
7	3	5	6	3	4	9345.105	-0.004
5	2	4	4	1	4	9576.832	0.012
8	2	7	7	2	6	9779.115	-0.023
7	2	5	6	2	4	9807.536	0.022
8	1	7	7	1	6	9813.902	-0.018
9	1	9	8	1	8	9986.950	-0.039
9	0	9	8	0	8	9987.270	-0.019
7	3	4	6	3	3	10252.012	0.017
8	4	5	7	4	4	10964.773	-0.049
5	5	1	4	4	0	11747.047	-0.030
5	5	0	4	4	1	11751.453	-0.028
11	0	11	10	1	10	12110.448	0.014
11	1	11	10	1	10	12110.449	-0.006
11	0	11	10	0	10	12110.449	-0.006
9	6	4	8	6	3	12407.779	-0.064
9	6	3	8	6	2	12438.142	-0.036
9	5	5	8	5	4	12453.432	-0.055

Table S5. Measured frequencies and residuals (in MHz) for the rotational transitions of rotamer III.

J'	K'_a	K'_c	J''	K''_a	K''_c	ν_{obs}	$\nu_{\text{obs}} - \nu_{\text{cal}}$
4	1	4	3	1	3	4545.419	-0.024
4	0	4	3	0	3	4702.383	0.044
4	2	3	3	2	2	4967.127	-0.013
4	3	2	3	3	1	5051.810	0.011
4	3	1	3	3	0	5073.861	-0.017
4	1	3	3	1	2	5303.830	0.014
5	0	5	4	0	4	5747.263	-0.008
5	2	4	4	2	3	6166.949	0.000
5	3	3	4	3	2	6324.875	-0.006
5	3	2	4	3	1	6398.732	0.019
5	1	4	4	1	3	6541.128	-0.004
5	2	3	4	2	2	6659.144	0.016
6	1	6	5	1	5	6718.127	0.002
6	0	6	5	0	5	6781.211	-0.012
6	2	5	5	2	4	7341.023	-0.004
6	3	4	5	3	3	7591.822	0.014
6	4	3	5	4	2	7602.326	-0.004
6	1	5	5	1	4	7708.113	0.002
6	3	3	5	3	2	7772.235	0.016
7	1	7	6	1	6	7785.900	-0.009
7	0	7	6	0	6	7819.113	-0.006
8	2	6	7	2	5	10634.589	-0.009
8	3	5	7	3	4	10639.478	-0.022
10	0	10	9	0	9	10962.328	0.013

Table S6. Cartesian coordinates (Å) of conformer of G-g+/cc/t at MP2/6-311++G (d,p).

Standard orientation

Center Number	Atomic Number	X	Y	Z
1	6	1.118048	-0.145818	-0.563114
2	6	0.787096	0.988689	0.413760
3	6	-0.711412	1.266401	0.434940
4	6	-1.502596	-0.017683	0.618177
5	6	-1.059200	-1.048126	-0.406765
6	1	0.914191	0.191206	-1.590965
7	1	1.117221	0.687765	1.412179
8	1	-0.945994	1.965053	1.248466
9	1	-1.304855	-0.438317	1.613794
10	1	-1.258241	-0.686377	-1.426503
11	8	0.324451	-1.304871	-0.262998
12	8	-1.022149	1.864834	-0.823539
13	1	-1.982528	1.955045	-0.850424
14	8	-2.875143	0.314795	0.458311
15	1	-3.359253	-0.518889	0.433817
16	8	1.506474	2.163259	0.076293
17	1	0.999140	2.588481	-0.627208
18	8	-1.769120	-2.220354	-0.133278
19	1	-1.562074	-2.857351	-0.825297
20	6	2.563285	-0.600470	-0.448769
21	1	3.220058	0.261649	-0.577329
22	1	2.768728	-1.333878	-1.239545
23	8	2.837434	-1.143909	0.833348
24	1	2.206706	-1.862380	0.954540

Table S7. Cartesian coordinates (\AA) of conformer of G+g-/cc/t at MP2/6-311++G (d,p).

Standard orientation

Center	Atomic	X	Y	Z
1	6	-1.164239	0.018263	0.146704
2	6	-0.516839	1.203280	-0.575394
3	6	0.980192	1.250356	-0.284278
4	6	1.627946	-0.106337	-0.512050
5	6	0.854062	-1.184442	0.228836
6	1	-1.090959	0.159855	1.234978
7	1	-0.665852	1.074937	-1.653618
8	1	1.456947	1.999983	-0.929331
9	1	1.597041	-0.358911	-1.580972
10	1	0.873260	-0.997441	1.312863
11	8	-0.487611	-1.194893	-0.221936
12	8	1.102038	1.637465	1.082886
13	1	2.038812	1.562519	1.302530
14	8	2.965238	-0.007628	-0.041448
15	1	3.328453	-0.900877	-0.055758
16	8	-1.134998	2.426948	-0.216766
17	1	-0.748175	2.677252	0.632343
18	8	1.457447	-2.403342	-0.090665
19	1	1.053526	-3.085764	0.455573
20	6	-2.615927	-0.179535	-0.241991
21	1	-2.673237	-0.331088	-1.329271
22	1	-3.185414	0.712576	0.021574
23	8	-3.194838	-1.270271	0.457195
24	1	-2.633776	-2.028782	0.263994

Table S8. Cartesian coordinates (Å) of conformer of Tg+/cc/t at MP2/6-311++G (d,p).

Standard orientation

Center	Atomic	X	Y	Z
1	6	1.006321	0.552649	0.192828
2	6	0.790054	-0.732964	-0.615001
3	6	-0.592248	-1.315107	-0.350621
4	6	-1.664620	-0.248362	-0.505890
5	6	-1.291411	0.990344	0.292328
6	1	0.982849	0.320976	1.267820
7	1	0.877185	-0.482897	-1.678469
8	1	-0.787339	-2.139156	-1.049664
9	1	-1.736893	0.053208	-1.559948
10	1	-1.242460	0.755092	1.366517
11	8	-0.034663	1.478965	-0.136356
12	8	-0.559488	-1.809202	0.986340
13	1	-1.464068	-2.067808	1.201907
14	8	-2.881743	-0.819837	-0.045901
15	1	-3.527518	-0.104236	-0.014242
16	8	1.798931	-1.700543	-0.338182
17	1	1.516546	-2.149229	0.470709
18	8	-2.271137	1.948703	0.022781
19	1	-2.067927	2.729754	0.548718
20	6	2.328533	1.234360	-0.139016
21	1	2.332926	2.226603	0.317634
22	1	2.405931	1.355463	-1.229237
23	8	3.437437	0.527192	0.388846
24	1	3.336301	-0.385510	0.090267

References

- 1 I. León, E. R. Alonso, S. Mata and J. L. Alonso, Shape of Testosterone, *J. Phys. Chem. Lett.*, 2021, **12**, 6983–6987.
- 2 E. R. Alonso, I. León and J. L. Alonso, in *Intra- and Intermolecular Interactions Between Non-covalently Bonded Species*, Elsevier, 2021, pp. 93–141.
- 3 M. Sanz-Novo, M. Mato, I. León, A. M. Echavarren and J. L. Alonso, Shape-Shifting Molecules: Unveiling the Valence Tautomerism Phenomena in Bare Barbaralones, *Angew. Chemie - Int. Ed.*, 2022, **61**, 1–6.
- 4 S. Mata, I. Peña, C. Cabezas, J. C. López and J. L. Alonso, A broadband Fourier-transform microwave spectrometer with laser ablation source: The rotational spectrum of nicotinic acid, *J. Mol. Spectrosc.*, 2012, **280**, 91–96.
- 5 J. L. Alonso and J. C. López, in *Top. Curr. Chem.*, 2014, vol. 364, p. 335.
- 6 Basic Terminology of Stereochemistry, <https://iupac.qmul.ac.uk/stereo/TZ.html>.
- 7 2018. Schrödinger Release 2018-3: Maestro Schrödinger, LLC, New York, NY, .
- 8 M. J. Frisch, G. W. Trucks, H. B. Schlegel, G. E. Scuseria, M. A. Robb, J. R. Cheeseman, G. Scalmani, V. Barone, G. A. Petersson, H. Nakatsuji, X. Li, M. Caricato, A. V. Marenich, J. Bloino, B. G. Janesko, R. Gomperts, B. Mennucci, H. P. Hratchian, J. V. Ortiz, A. F. Izmaylov, J. L. Sonnenberg, D. Williams-Young, F. Ding, F. Lipparini, F. Egidi, J. Goings, B. Peng, A. Petrone, T. Henderson, D. Ranasinghe, V. G. Zakrzewski, J. Gao, N. Rega, G. Zheng, W. Liang, M. Hada, M. Ehara, K. Toyota, R. Fukuda, J. Hasegawa, M. Ishida, T. Nakajima, Y. Honda, O. Kitao, H. Nakai, T. Vreven, K. Throssell, J. J. A. Montgomery, J. E. Peralta, F. Ogliaro, M. J. Bearpark, J. J. Heyd, E. N. Brothers, K. N. Kudin, V. N. Staroverov, T. A. Keith, R. Kobayashi, J. Normand, K. Raghavachari, A. P. Rendell, J. C. Burant, S. S. Iyengar, J. Tomasi, M. Cossi, J. M. Millam, M. Klene, C. Adamo, R. Cammi, J. W. Ochterski, R. L. Martin, K. Morokuma, O. Farkas, J. B. Foresman and D. J. Fox, 2016, Gaussian 16, Revision B.01, Gaussian, Inc., Wallin.
- 9 C. Møller and M. Plesset, Note on an Approximation Treatment for Many-Electron Systems, *Phys. Rev.*, 1934, **46**, 618–622.
- 10 A. D. Becke, A new mixing of Hartree–Fock and local density-functional theories, *J. Chem. Phys.*, 1993, **98**, 1372–1377.
- 11 S. Grimme, J. Antony, S. Ehrlich and H. Krieg, A consistent and accurate ab initio parametrization of density functional dispersion correction (DFT-D) for the 94 elements H–Pu, *J. Chem. Phys.*, 2010, **132**, 154104.
- 12 S. Grimme, S. Ehrlich and L. Goerigk, Effect of the damping function in dispersion corrected density functional theory, *J. Comput. Chem.*, 2011, **32**, 1456–1465.
- 13 E. R. Johnson and A. D. Becke, A post-Hartree-Fock model of intermolecular interactions: Inclusion of higher-order corrections, *J. Chem. Phys.*, 2006, **124**, 0–9.
- 14 M. J. Frisch, J. A. Pople and J. S. Binkley, Self-consistent molecular orbital methods 25. Supplementary functions for Gaussian basis sets, *J. Chem. Phys.*, 1984, **80**, 3265–3269.